

# An X-ray Fourier line shape analysis in cold-worked hexagonal zirconium

S. K. CHATTERJEE, S. P. SEN GUPTA

*Department of General Physics and X-rays, Indian Association for the Cultivation of Science, Calcutta 700032, India*

Detailed Fourier analysis of line shapes has been carried out in hexagonal zirconium metal in the cold-worked and partially recovered states. X-ray diffraction profiles from the fault-unaffected 10.0, 00.2, 11.0, 11.2 and 00.4 and fault-affected 10.1, 10.3, 20.1, 10.2 and 20.2 reflections have been recorded using a counter diffractometer for this purpose. The line shape analysis has shown small anisotropy as regards the domain sizes and strains, the average values being of the order of 280 Å and  $2.08 \times 10^{-3}$  respectively in the cold-worked state with a small recovery at a higher temperature. Least-square solution applied to fault-affected reflections has yielded very small concentration of deformation faults with a negligible proportion of growth faults. Results are found to be consistent with earlier X-ray measurements and recent electron microscope investigations on zirconium.

## 1. Introduction

X-ray diffraction studies of cold-worked metals and alloys have received considerable attention in recent years [1-3] as these studies enable one to get a detailed picture of the deformed state. Quantitative estimates of coherent domain sizes, microstrains within these domains, stacking fault probability, density of dislocations, etc. can be obtained from the several existing methods of analyses, namely, Warren-Averbach's Fourier analysis of line shapes [1-3], integral breadth measurements [2, 3] and variance analysis [4, 5]. Of these, Fourier analysis of line shapes [2] appears to be more effective as it brings out the relative contributions of stacking fault concentrations, small particle sizes and microstrains to the observed broadening effect as well as the variation of strain with distance and, hence, has been widely used in obtaining the microstructural parameters of the deformed state.

Although a considerable amount of work has already been performed in fcc metals and alloys utilizing X-ray diffraction methods [3, 6-8], relatively few studies have so far been performed in hexagonal close-packed materials [3, 9-15]. As such there has been growing interest in recent years in the study of hexagonal metals utilizing both transmission electron microscopy [16-19] and X-ray diffraction analysis [20-22] in

order to elucidate the incidence of faulting and, hence, the dislocation structure responsible for the deformation mechanism in these materials. However, as far as X-ray studies are concerned, the analyses are rather incomplete in the sense that these have been made in most of the cases by considering the effects of deformation on fewer diffraction profiles from which it is not possible to obtain all the microstructural parameters in a consistent way and, hence, a fairly accurate picture of the deformed state [10, 11, 14, 20-22]. It thus seems necessary to carry out a detailed analysis of line shapes in hexagonal metals considering the effects of deformation on the maximum number of observable reflections in order to obtain a fairly representative picture of the deformed condition of the material in terms of the microstructural parameters, which are the manifestations of the dislocation structure resulting from the deformation process. In view of this, we have undertaken a programme for detailed and systematic study with hexagonal metals of importance. The present investigation deals with hexagonal zirconium, and detailed Fourier analysis of line shapes [1, 2] has been performed considering fault-unaffected 10.0, 00.2, 11.0, 11.2, 00.4 reflections and fault-affected 10.1, 10.3, 20.1, 10.2, 20.2 reflections from cold-worked (at room temperature) and

partially recovered (annealed at 550°C for 18 h) states of zirconium. Recent electron microscope investigations of zirconium [18, 19] have also revived considerable interest in the study of the microstructure of this metal in particular.

## 2. Experimental procedure

Cold-working was achieved at room temperature ( $29 \pm 1^\circ\text{C}$ ) by careful hand-filing of the spectroscopically pure zirconium rod (3 mm diameter) supplied by Messrs Johnson, Matthey & Co Ltd, London. The filings were sieved through a 250 mesh screen and a sample of the filings was retained in the "as-filed" condition representing the "cold-worked" state. Besides this, one sample was prepared by annealing the filings at 800°C for 12 h in an evacuated quartz capsule representing the "fully annealed" state as observed from the sharpness and splitting of  $K\alpha_1 - \alpha_2$  doublet at low angles and another similarly annealed at 550°C for 18 h representing the "partially recovered" state. The diffractometer samples were prepared in the usual way using a solution of Canada balsam in xylene as a binder [6]. The line profiles were recorded using the Philips Geiger Counter Diffractometer (PW 1050, 1051) with nickel filtered  $\text{CuK}\alpha$ -radiation from a stabilized Philips X-ray Generator (PW 1010) operating at 30 kV and 16 mA. A chart recording was initially made followed by point counting at intervals of  $0.1^\circ$  in  $2\theta$  for the general background, decreasing to  $0.01^\circ$  in  $2\theta$  near the maxima of the peaks, where  $\theta$  is the Bragg angle [6]. All the measurements were carried out at room temperature ( $29 \pm 1^\circ\text{C}$ ). The line profiles from the sample representing the "fully annealed" state were taken as standard for the correction of the instrumental broadening employing Stokes' method [23]. Altogether ten diffraction profiles, namely 10.0, 00.2, 11.0, 11.2, 00.4, 10.1, 10.2, 10.3, 20.1 and 20.2 from the cold-worked, partly annealed and fully annealed samples were recorded and taken into consideration for the present investigation. It was not possible to measure 20.0 and other higher orders of the fault-affected reflections excepting 10.1 because of considerable degree of overlap and diffuseness. The tails of the overlapped profiles (11.2 and 20.1) were recovered by assuming a symmetrical intensity distribution about the peak [9, 12]. Owing to considerable overlap in certain profiles, the separation of  $\alpha_1 - \alpha_2$  doublet by the graphical method of Rachinger [24] was not made.

Mogard and Averbach [10] in their studies with Zr have considered  $\{100\}$   $\{101\}$  and  $\{002\}$  reflections from the samples cold-worked at room temperature and annealed at 600°C for 3 h. Lele and Anantharaman [21] have performed the analysis with Zr considering only 0002,  $10\bar{1}1$  and  $10\bar{1}2$  reflections from the samples cold-worked at 25°C and annealed at several temperatures, namely, 275, 550 and 800°C for 2 h.

## 3. Fourier analysis of line shapes

The line shape analysis as outlined by Warren [2] has been adopted for the quantitative estimates of coherent domain or particle sizes, lattice strains, deformation and growth stacking faults which characterize the cold-worked state. The entire analysis is based on basal slip, i.e. slip on 00.2 planes of the hcp structure. By considering each reflection  $H K \cdot L_0$  as a  $00l'$  reflection in terms of orthorhombic axes, the power distribution per unit arc length is described by a Fourier series in terms of a position in reciprocal space and is expressed as:

$$p'_{2\theta} = k' \sum A_n^S A_n^D \cos 2\pi n (h_3' - l') \quad (1)$$

in which  $h_3' - l' = 2 | \bar{a}_3' | (\sin \theta - \sin \theta_0)/\lambda$  where  $| \bar{a}_3' |$  is a fictitious distance chosen to correspond to the  $\sin \theta$  interval within which the peak is expressed as a Fourier series.  $A_n^S$  and  $A_n^D$  represent the size and distortion coefficients respectively,  $A_n^S$  includes the effects of both domain size and faulting. Expressing (1) in terms of a length  $L (= n | \bar{a}_3' |)$  which has the significance of a distance normal to the reflecting planes, the distortion coefficient for a gaussian strain distribution is given by:

$$A_L^D = \exp(-2\pi^2 L^2 \langle \epsilon_L^2 \rangle / d^2), \quad (2)$$

where  $\langle \epsilon_L^2 \rangle$  is the mean-square strain and  $d$  is the interplanar spacing of the reflecting planes.

The separation of particle size coefficient,  $A_L^S$ , and distortion coefficient,  $A_L^D$ , is usually done by the use of multiple orders where a log plot of Fourier coefficients  $A_L (= A_L^S \cdot A_L^D)$  against  $1/d^2$  is made and the intercept and slope of this plot yield  $A_L^S$  and  $A_L^D$  as a function of  $L$ . The values of  $A_L^D$  gives directly the rms strain  $\langle \epsilon_L^2 \rangle^{\frac{1}{2}}$  from Equation 2 and the initial slopes of the plots of  $A_L^S$  against  $L$  are related by the following three equations [2]:

$$H - K = 3N \quad : \quad - \left( \frac{dA_L^S}{dL} \right)_0 = \frac{1}{D} \quad (3)$$

$$\begin{aligned}
 H - K = 3N \pm 1, L_0 \text{ (even)}: & - \left( \frac{dA_L^S}{dL} \right)_0 \\
 = \frac{1}{D_{\text{effective}}} = \frac{1}{D} + \frac{|L_0|d}{C^2} (3\alpha + 3\beta) & \quad (4)
 \end{aligned}$$

$$\begin{aligned}
 H - K = 3N \pm 1, L_0 \text{ (odd)}: & - \left( \frac{dA_L^S}{dL} \right)_0 \quad (5) \\
 = \frac{1}{D_{\text{effective}}} = \frac{1}{D} + \frac{|L_0|d}{C^2} (3\alpha + \beta) &
 \end{aligned}$$

where  $N$  is zero or an integer,  $D$  is the average domain size (true) normal to the reflecting planes,  $C = 2d_{00.2}$ , and  $\alpha$  and  $\beta$  are the deforma-

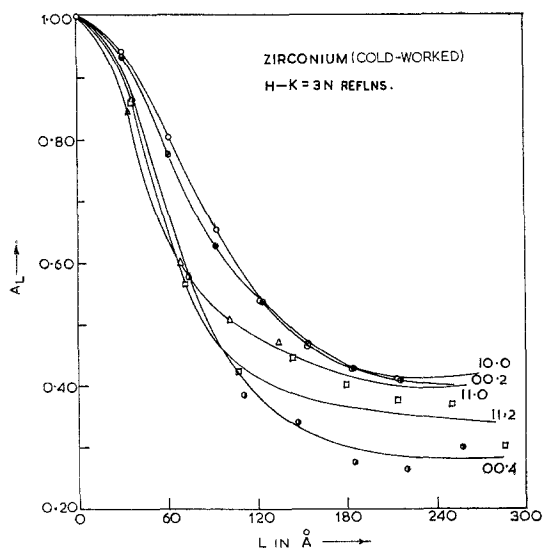


Figure 1 Fourier coefficients  $A_L$  versus  $L$  for  $H - K = 3N$  reflections for cold-worked (room temperature  $29 \pm 1^\circ\text{C}$ ) zirconium.

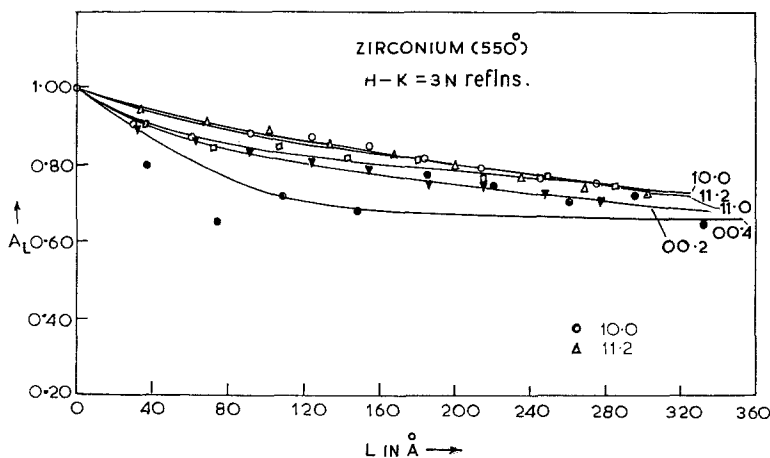


Figure 2 Fourier coefficients  $A_L$  versus  $L$  for  $H - K = 3N$  reflections for partially recovered (annealed at  $550^\circ\text{C}$  for 18 h) zirconium.

tion and growth fault probabilities respectively. The second terms in Equations 4 and 5 represent the fictitious domain size due to stacking faults.

In the present analysis, Stokes' corrected [23] normalized Fourier coefficients for the cold-worked and partially recovered samples of Zr were obtained using a computer program written for IBM 1130. Log plots were made for the fault-unaffected reflections only (i.e.  $H - K = 3N$ ) due to the absence of higher orders with  $L_0$  only odd or only even (i.e. for  $H - K = 3N \pm 1$ ). As such it was considered that the effects of both domain size and strains remain the same for the fault-unaffected and fault-affected reflections [9, 12, 13, 15, 20-22]. From the mean-square strain values for the reflections with  $H - K = 3N$ , the distortion coefficients  $A_L^D$  were obtained from Equation 2 which were then utilized for the determination of the effective size coefficients  $A_L^S$  for the reflections with  $H - K = 3N \pm 1$ . From the initial slopes and the average domain size,  $D$ , obtained from log plots, the values of  $\alpha$  and  $\beta$  were determined from a least-square solution of five sets of values arising from Equations 4 and 5.

#### 4. Results and discussion

Stokes' corrected Fourier coefficients  $A_L$  as a function of  $L$  for the reflections with  $H - K = 3N$  and  $H - K = 3N \pm 1$  ( $L_0$  odd and even) for the cold-worked and partially annealed zirconium have been plotted in Figs. 1 to 4. The partial recovery of the sample is clearly observed in Figs. 2 and 4 which show an upward trend in the coefficients. The values of average domain

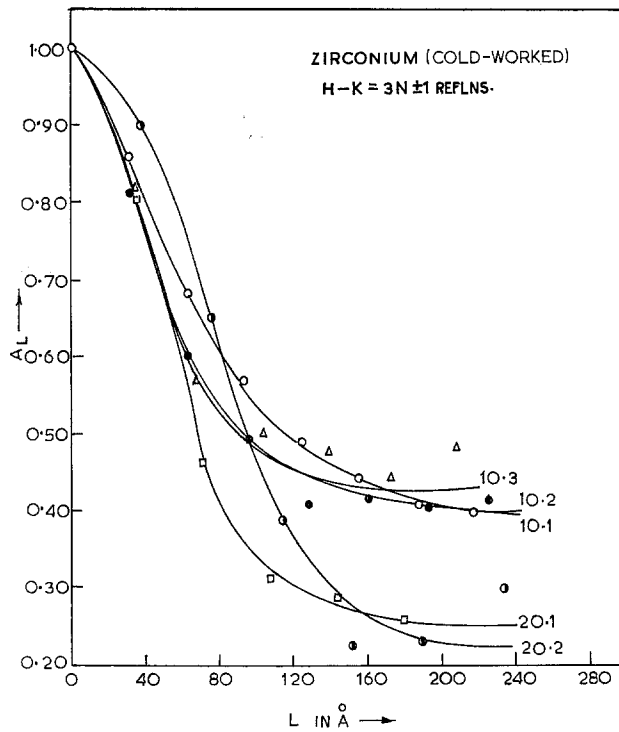


Figure 3 Fourier coefficients  $A_L$  versus  $L$  for  $H - K = 3N \pm 1$  reflections for cold-worked zirconium.

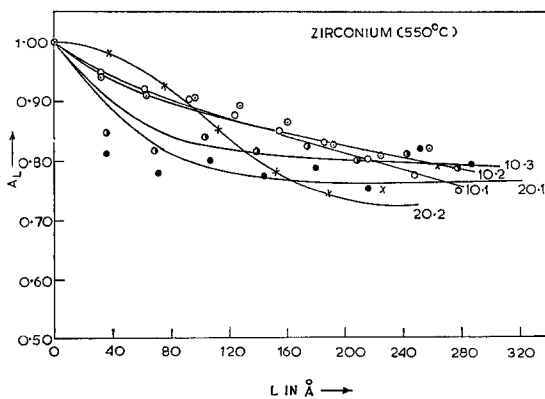


Figure 4 Fourier coefficients  $A_L$  versus  $L$  for  $H - K = 3N \pm 1$  reflections for partially recovered zirconium.

sizes,  $D$ , and rms strains,  $\langle \epsilon_L^2 \rangle^{\frac{1}{2}}$ , at an averaging distance of  $L = 100 \text{ \AA}$  obtained from the log plots of 10.0, 00.2, 11.0, 11.2, 00.4 reflections which reflect a considerable degree of isotropy up to  $L = 150 \text{ \AA}$  (Fig. 5) have been shown in Table I. The results of Mogard and Averbach [10] for zirconium also show considerable isotropy in domain sizes, e.g. 370, 340 and 330  $\text{\AA}$  respectively. Lele and Anantharaman's Fourier analysis [21] considering single reflection has

also shown similar tendency. However, the present analysis with five fault-unaffected reflections has indicated clearly the smallness in anisotropy. The value of the average domain size obtained from the present measurement is 280  $\text{\AA}$  for the cold-worked state and for the partially recovered zirconium, the domain size value is about 500  $\text{\AA}$  which shows a small recovery effect in the fragmentation of domains. As regards rms strains the present value of  $2.08 \times 10^{-3}$  at an average distance of  $L = 100 \text{ \AA}$  for the cold-worked state compares satisfactorily with those observed earlier [10, 21]. A decrease in the strain values ( $0.71 \times 10^{-3}$ ) has been found to occur for the sample annealed at 550°C for 18 h showing considerable removal of strain from the sample. The variation of rms strains,  $\langle \epsilon_L^2 \rangle^{\frac{1}{2}}$ , over the variation of column length,  $L$ , as shown in Fig. 6 is quite consistent with the dislocation structure that develops in deformed metals and alloys and has been observed earlier in most of the studies with cold-worked fcc and hcp metals and alloys [3, 6-9, 20].

For the fault-affected reflections with  $H - K = 3N \pm 1$ , the plots of the size coefficients  $A_L^S$  as function of  $L$  obtained after correcting for distortion effects for the cold-worked and

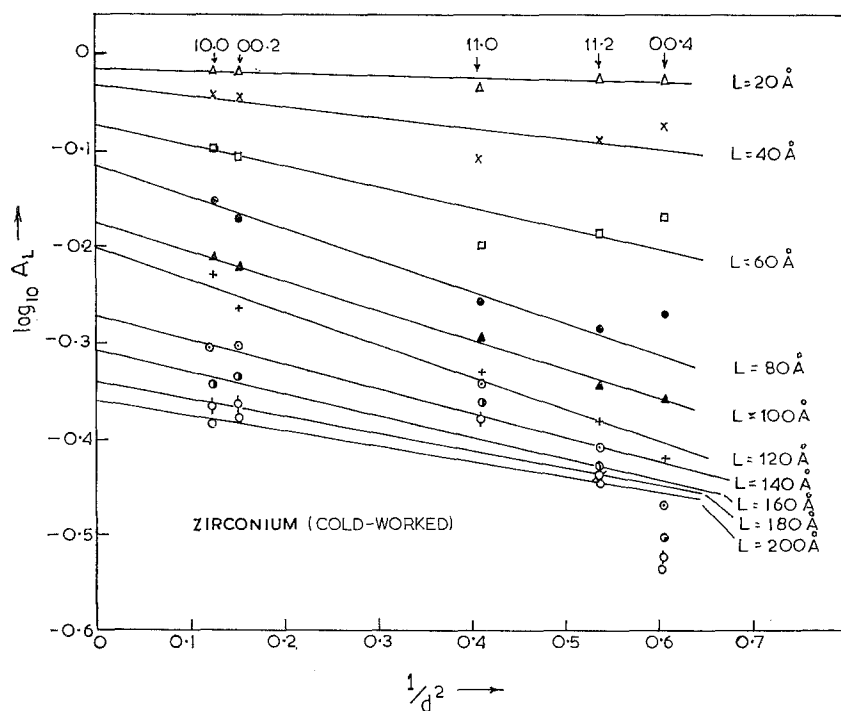


Figure 5 Plot of  $\log_{10} A_L$  versus  $1/d^2$  for values of  $L$  in cold-worked zirconium.

partially recovered zirconium samples (Figs. 7 and 8) show, to some extent, the "hook effect" [1, 2] which is particularly prominent for the 20.1 reflection and arises in the line shape analysis due to uncertainty in the background estimation. The values of the effective particle sizes,  $D_e$  ( $D_{\text{effective}}$ ) determined from the initial straight line portion of the above plots (Table II) are found to be quite close to the average domain size value  $D$  (Table I) suggesting very small particle size effect (fictitious) from the stacking fault concentrations. This is also apparent from the variation of coefficients  $A_L$  with  $L$  (Figs. 1 to 4) where the coefficients  $A_L$  for the reflections with  $H - K = 3N \pm 1$  do not decrease rapidly

with  $L$  and vary more or less in a similar manner. The rapid decrease of  $A_L$  usually gives an indication of stacking fault effects [9, 12, 13]. The above observation is true for both the cold-worked and partially recovered samples of zirconium. Mogard and Averbach [10], using the method of multiple order, have obtained for the  $\{101\}$  reflections the effective particle size value very close to those for the fault-unaffected reflections leading to the conclusion that the probability of occurrence of stacking faults is less in deformed zirconium. It may, however, be mentioned that the size coefficients,  $A_L^S$ , for 10.1 and 20.2 reflections are to be equated by two different equations namely, Equations 4 and

TABLE I Average domain size  $D$  and rms strain  $\langle \epsilon_L^2 \rangle_{L=100\text{\AA}}^{1/2}$  in hexagonal zirconium from fault-unaffected reflections

Reflections ( $H - K = 3N$ )	Cold-worked		Annealed at 550°C for 18 h	
	$D$ (Å)	$\langle \epsilon_L^2 = 100 \text{\AA} \rangle^{1/2} \times 10^3$	$D$ (Å)	$\langle \epsilon_L^2 = 100 \text{\AA} \rangle^{1/2} \times 10^3$
10.0				
00.2				
11.0	280	2.08	500	0.71
11.2				
00.4				

TABLE II Effective particle size,  $D_e$ , and fault probabilities ( $\alpha$  and  $\beta$ ) in hexagonal zirconium from fault-affected reflections

Reflections ( $H - K = 3N \pm 1$ )	$D_e$ (Å)		$(3\alpha + \beta) \times 10^3$		$(3\alpha + 3\beta) \times 10^3$	
	Cold-worked	Annealed at 550°C	Cold-worked	Annealed at 550°C	Cold-worked	Annealed at 550°C
$L_0$ odd						
10.1	244	492	5.64	0.32		
10.3	274	418	0.47	2.33		
20.1	190	392	32.70	10.67		
$L_0$ even						
10.2	201	486			9.75	0.42
20.2	186	482			19.30	0.75

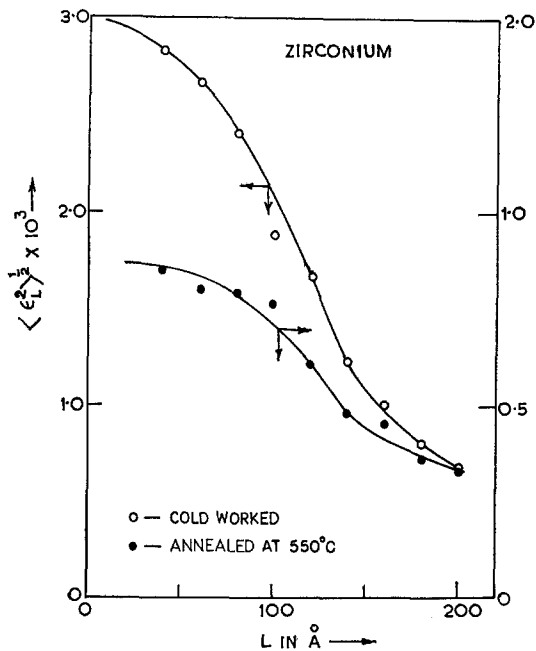


Figure 6 Rms strain  $\langle \epsilon_L^2 \rangle^{1/2}$  versus  $L$  for cold-worked and partially recovered zirconium.

5 in which the fault effects are also different, and this has not been considered in the above study.

The compound fault probabilities  $(3\alpha + \beta)$  and  $(3\alpha + 3\beta)$  which have been obtained from Equations 4 and 5 using the isotropic domain size value  $D$  are shown in Table II for the five fault-affected reflections of the respective cold-worked and partially recovered states of the sample. A least-square analysis has been found to yield very small values for the deformation fault probability  $\alpha$  ( $\alpha$  being  $\sim 4 \times 10^{-3}$  and  $\sim 2 \times 10^{-3}$  for the cold-worked and partially recovered states respectively). The occurrence of

growth faults seems to be negligible as apparent from the values of  $\beta$  which, for the cold-worked state, is  $< 1 \times 10^{-3}$  and for the partially recovered state becomes negative. Thus,  $\beta$  may as well be considered as zero in agreement with the earlier observations in plastically deformed hcp metals and alloys [9, 12, 13, 20, 21]. With this consideration, the values of deformation fault probability  $\alpha$  for the respective planes are also calculated and shown in Table II. When

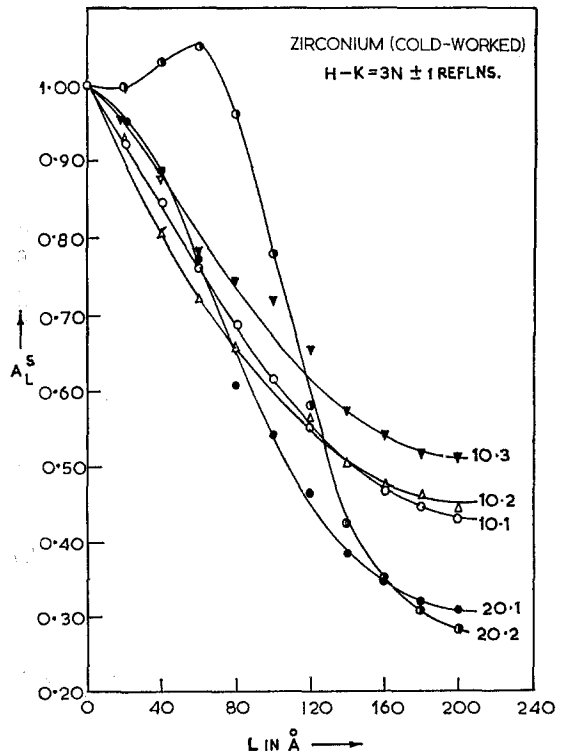


Figure 7 Distortion corrected size coefficients  $A_L^S$  versus  $L$  for  $H - K = 3N \pm 1$  reflections for cold-worked zirconium.

TABLE II Effective particle size,  $D_e$ , and fault probabilities ( $\alpha$  and  $\beta$ ) in hexagonal zirconium from fault-affected reflections

Least square solution				$\alpha \times 10^3$ (assuming $\beta = 0$ )		Mean $\alpha \times 10^3$	
$\alpha \times 10^3$		$\beta \times 10^3$		Cold-worked	Annealed at 550°C	Cold-worked	Annealed at 550°C
Cold-worked	Annealed at 550°C	Cold-worked	Annealed at 550°C	Cold-worked	Annealed at 550°C	Cold-worked	Annealed at 550°C
4.07	2.12	0.77	-1.93	1.88 0.16 10.90	0.11 0.78 3.55	4.52	0.97
				3.25 6.43	0.14 0.25		

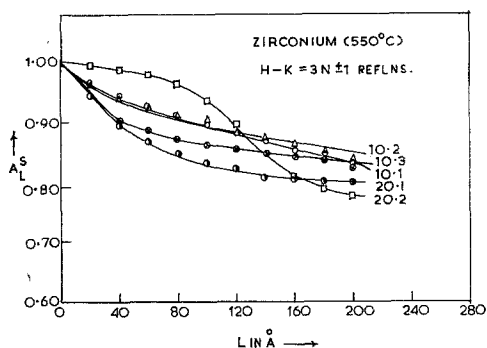


Figure 8 Distortion corrected size coefficients  $A_L^S$  versus  $L$  for  $H - K = 3N \pm 1$  reflections for partially recovered zirconium.

only  $\alpha$  is considered, it may be seen that 20.1 and, to some extent, 20.2 planes are slightly affected by deformation faults. The recovery effect is also observed for the respective planes. The above findings, along with the considerations of experimental errors and the small anisotropy in domain sizes and strains, are more or less consistent with the earlier ones by Mogard and Averbach [10] and Lele and Anantharaman [21] who were unable to detect any presence of stacking faults. A detailed analysis has not been performed in the above studies in predicting the stacking fault effects. The very small concentration of deformation faults as observed here is, however, quite possible from several considerations. As there exists an inverse relation between fault probability and fault energy, the low value of  $\alpha$  implies rather a high stacking fault energy considering the dislocation density in the deformed material to be  $\sim 10^{11} \text{ cm}^{-2}$ . The theoretical estimates of Seeger [25] from the considera-

tion of electronic structure also predict a high fault energy for this hexagonal metal. It is further known that the deformation by slip in hcp metals primarily occurs in the close-packed direction and the primary slip plane may be either basal  $\{0002\}$  or the first-order prism  $\{10\bar{1}0\}$  planes governed essentially by the stacking fault energy [26]. Recent electron microscope observations [18, 19] in single crystals of zirconium deformed in tension have shown that the first-order prismatic slip happens to be the easiest slip mode, the stacking fault energy on the prism planes being  $56 \text{ erg cm}^{-2}$  while the tendency of basal slip increases with temperature. This, however, contradicts the earlier observation [26] that the basal slip must be favoured in hcp metals since in case of prismatic slip the energy of the stacking fault formed is expected to be high due to a change in co-ordination number and increase in the spacing between the corrugated  $\{10\bar{1}0\}$  planes in the metastable position. Since the entire line shape analysis in hexagonal systems is based on an X-ray diffraction theory considering basal slip only [1, 2] the very low stacking fault probability in zirconium, as determined in the present line shape analysis, appears to be quite reasonable in the light of above considerations.

## 5. Conclusions

From a detailed Fourier analysis of line shapes for the cold-worked and partially recovered states of Zr the following conclusions may be tentatively drawn.

1. Small anisotropy in the domain sizes and strains have been observed from the log plots of five fault-unaffected reflections. This justifies the assumption that the influences of both

domain size (true) and strain remain uniform for all the observed reflections.

2. Very small concentration of deformation stacking faults occurs in the material, whereas the growth faults do not appear to exist in conformity with the observations made in plastically deformed hcp metals and alloys.

3. Results are consistent with the earlier X-ray measurements and also recent electron microscope observations on deformed single crystals of zirconium. In this material, the basal slip appears to be inhibited by the prismatic slip mode.

### Acknowledgement

The authors are thankful to Professor A. K. Barua for his active interest in this work.

### References

1. B. E. WARREN, *Prog. Metal Phys.* **8** (1959) 147.
2. *Idem*, "X-ray Diffraction" (Addison-Wesley, Reading, Mass., 1972).
3. C. N. J. WAGNER, "Local Atomic Arrangements studied by X-ray Diffraction", edited by J. B. Cohen and J. E. Hilliard (Gordon and Breach, 1966, New York) Chapter 6.
4. A. J. C. WILSON, *Proc. Phys. Soc. (London)* **80** (1962) 286.
5. J. I. LANGFORD and A. J. C. WILSON, "Crystallography and Crystal Perfection", edited by G. N. Ramachandran (Academic Press, London, 1963) p. 207.
6. S. P. SEN GUPTA and M. A. QUADER, *Acta Cryst.* **20** (1966) 798.
7. S. P. SEN GUPTA, *ibid* **23** (1967) 244.
8. S. P. SEN GUPTA and M. DE, *J. Phys. Soc. Japan* **29** (1970) 360.
9. R. P. STRATTON and W. J. KITCHINGMAN, *Brit. J. Appl. Phys.* **16** (1965) 1311.
10. J. H. MOGARD and B. L. AVERBACH, *Acta Metallurgica* **6** (1958) 552.
11. J. SPREADBOROUGH and J. W. CHRISTIAN, *Proc. Phys. Soc. (London)* **74** (1959) 609.
12. S. P. SEN GUPTA and K. N. GOSWAMI, *Brit. J. Appl. Phys.* **18** (1967) 193.
13. M. DE and S. SEN, *ibid J. Phys. D* **1** (1968) 1141.
14. G. B. MITRA and N. K. MISRA, *Acta Cryst.* **22** (1967) 454.
15. M. DE and S. P. SEN GUPTA, *J. Appl. Cryst.* **6** (1973) 237.
16. P. B. PRICE, "Electron Microscopy and Strength of Crystals", edited by G. Thomas and J. Washburn (Interscience, New York, 1963) Chapter 2.
17. S. MADER, *ibid*, Chapter 4.
18. A. AKHTAR and E. TEGHTSOONIAN, *Acta Metallurgica* **19** (1971) 655.
19. A. AKHTAR, *ibid* **21** (1973) 1.
20. S. LELE and T. R. ANANTHARAMAN, *Z. Metallk.* **58** (1967) 37.
21. *Idem*, *ibid* **58** (1967) 461.
22. R. K. GUPTA, P. RAMARAO and T. R. ANANTHARAMAN, *ibid* **63** (1972) 575.
23. A. R. STOKES, *Proc. Phys. Soc. (London)* **61** (1948) 382.
24. W. A. RACHINGER, *J. Sci. Instrum.* **25** (1948) 254.
25. A. SEEGER, "Dislocation and Mechanical Properties of Crystals" (New York: John Wiley & Sons, London: Chapman and Hall, 1957) p. 243.
26. W. TYSON, *Acta Metallurgica* **15** (1967) 574.

Received 10 September and accepted 27 November 1973.